Virginia Commonwealth University
VCU Scholars Compass

Theses and Dissertations

Graduate School

2015

Risperidone and its Deconstructed Analogs: Functional Effects on the 5HT2AR

Sneha Shah
Virginia Commonwealth University, shahsr2@vcu.edu

Follow this and additional works at: http://scholarscompass.vcu.edu/etd

Part of the Medical Physiology Commons

Downloaded from

http://scholarscompass.vcu.edu/etd/3792

Risperidone and its Deconstructed Analogs: Functional Effects on the 5HT2AR

A thesis submitted in partial fulfillment of the requirements for the degree of Master of Science at Virginia Commonwealth University

By

Sneha Shah
B.A. University of Virginia, Charlottesville, VA, 2013

Director: DIOMEDES E. LOGOTHETIS
CHAIR, DEPARTMENT OF PHYSIOLOGY AND BIOPHYSICS

Virginia Commonwealth University
Richmond, Virginia
April 2015

ACKNOWLEDGEMENTS

First and foremost, I would like to thank my thesis mentor, Dr. Diomedes Logothetis, for his leadership, guidance and encouragement throughout the development of the project. He has been absolutely supportive of my experience in the past year, never ceasing to amaze me with his patience and resourcefulness. I would also like to extend my thanks to my committee members, Dr. Richard Glennon and Dr. Srinivasa Karnam, who have also been supportive throughout this process. Special thanks goes to Dr. Lia Baki and Dr. Jose Miguel Eltit whose expert help with cell culture proved necessary for additional experiments for my Masters dissertation. My gratitude extends to my graduate student mentor, Jason Younkin, who has greatly shaped my scientific understanding of GPCRs and electrophysiology, in addition to technical training.

I would also like to thank my colleagues and good friends, Amr Ellaithy, Candice-Hatcher Solis, Guoqing Xiang and Junghoon Ha, for providing me with tremendous support and enabling me to think critically about my experiments as well as giving me moral support. They have challenged my thinking and kept filling me with ideas. I want to thank all of the other laboratory members of the Logothetis lab who were readily available to provide me with technical support and counsel.

To Farrell Irons and Alexandra Hoffman, my current roommates, thank you for listening, offering me advice, and supporting me through this entire process. Lastly, and most importantly, I would like to thank my parents, Sangeeta and Rupen Shah and my sister, Asmita Shah. Without their unconditional love, I would not be where I am today.

TABLE OF CONTENTS

Chapter

LIST OF FIGURES

LIST OF ABBREVIATIONS

DNA   Deoxyribonucleic acid

DMEM   Dulbecco's modified Eagle's medium

FBS   Fetal bovine serum

FURA2   Ratiometric fluorescent dye

GDP   Guanosine diphosphate

GIRK   G protein-gated inwardly rectifying K^+ channel

GPCR   G protein-coupled receptor

GTP   Guanosine-5'-triphosphate

HEPES   4-(2-hydroxyethyl)-1-piperazineethanesulfonic acid

Kir   Inwardly-rectifying potassium channel

PBS   Phosphate buffered saline

PIP$_2$ Phosphatidylinositol-4,5-bisphosphate

PLC   Phospholipase C

RHV   Initials of Rakesh Vekariya, a previous student who synthesized the deconstructed analogs initially

5HT2AR   5-hydroxytryptamine receptor 2A

5-HT   5-hydroxytryptamine

ABSTRACT

Risperidone and its Deconstructed Analogs: Functional Effects on the 5HT2AR

By: Sneha Shah, B.A.

A thesis submitted in partial fulfillment of the requirements for the degree of Master of Science at Virginia Commonwealth University

Virginia Commonwealth University, 2015
Thesis Director: Diomedes E. Logothetis, Ph.D.
Chair, Department of Physiology and Biophysics

G protein-coupled receptors (GPCRs) are seven-transmembrane domain receptors that sense extracellular signal and activate intracellular signaling pathways. The serotonin 5HT2A receptor (or 2AR) is one of the GPCRs coupled to Gq proteins, activating PLC and hydrolyzing PIP2. This hydrolysis causes a diffusion of bound PIP2 away from the channel binding site resulting in G protein-gated inwardly rectifying K^+ channel (GIRK) inhibition and a downstream stimulation of Ca^{2+} release from endoplasmic reticulum stores. Previous experiments have demonstrated that the serotonin 5HTA receptor is a target of serotonergic psychedelic drugs, such as LSD, and partially mediates the action of many atypical antipsychotic drugs. However, the portion responsible for the functional activity and response of these drugs is unknown. The purpose of this study was to functionally characterize four deconstructed analogs of risperidone, an atypical antipsychotic agent, using two assays: by application to $5HT_{2A}$ receptors in *Xenopus* oocytes and by calcium epifluorescence imaging in a HEK293 cell line stably expressing 2AR. Our experiments revealed that two analogs, RHV-006 and RHV-008, are partial agonists by themselves and greatly antagonize the effects of serotonin. RHV-006 and RHV-008 contain the piperidine and benzisoxizole ring systems of risperidone. RHV-023 and RHV-026, on the other hand, are more efficacious agonists than RHV-006 and RHV-008 but display a non-antagonistic effect with serotonin. RHV-023 and RHV-026 contain both the piperidine and benzisoxizole ring systems in addition to part of the diazabicyclo ring, thus containing more of risperidone's structure than RHV-006 and RHV-008.

INTRODUCTION

G- Protein- Coupled Receptors (GPCRs) and their downstream signaling partners constitute one of the largest classes of molecular targets contributing to many diseases. Half the current drugs on the market target GPCRs, generating tens of billions of dollars in revenue and representing a significant portion of the portfolio of many pharmaceutical companies (Solis, et al, 2014). Approximately 80% of known hormones and neurotransmitters activate cellular signal transduction mechanisms by activating GPCRs (Birnbaumer et al., 1990). Due to their importance, GPCRs and their signaling have been studied extensively and breakthroughs in our understanding of how their work has received multiple Nobel Prizes (Lin, 2013).

GPCRs are transmembrane receptors with an extracellular N terminus, a cytoplasmic C terminus and 7 transmembrane helices connected by loops (Ballesteros and Weinstein, 1994). GPCRs sense molecules outside the cell and activate intracellular signal transduction through pathways involving activation of G- proteins (Lefkowitz, 2007). These heterotrimer G (G-alpha-beta-gamma) proteins transduce ligand binding of the receptor to downsteam effectors. The cycle is described in three steps. The first occurs when binding of the ligand to the GPCR induces a conformational change to the receptor that is transduced to the Galpha subunit, such that its affinity for intracellular GTP is greatly increased over the already bound GDP, and in a Mg^{2+} dependent manner GDP is exchanged with GTP. The activated GPCR is acting as a guanine nucleotide exchange factor (GEF) to stimulate the exchange of nucleotides with the G- alpha subunit. Second, the G-alpha subunit uses the binding energy of GTP to produce a conformation favoring its dissociation from G-beta-gamma and association with effector proteins. Similarly, the dissociated Gbeta-gamma can also interact with effectors. Third, the activation of G- protein subunits ends by hydrolysis of GTP to GDP by the GTPase activity of the G-alpha subunit,

enabling re-association with Gbeta-gamma. Following re- association, the heterotrimeric G-protein can interact again with GPCRs and the activation cycle can continue (Solis, et al, 2014).

Co-expression of GPCRs with an inwardly rectifying potassium (Kir) channel reporter allows for membrane-delimited G- protein signaling, and its quantification can be achieved through measurement of ionic currents. Kir channels are named for their ability to conduct K^+ ions better in the inward ($V_m < E_k$) rather than the outward ($V_m > E_k$) direction (Hibino *et al.*, 2010). Assessment of Gq signaling in oocytes involves co-expression of a Gq-coupled GPCR with a channel reporter, followed by ligand-induced hydrolysis of PIP2 resulting in current inhibition (Figure 2). Kir activity is highly dependent on interactions with PIP2 to maintain its activity. Stimulation of the Gq coupled GPCR by the appropriate ligand leads to activation of PLC and hydrolysis of PIP2 to inositol triphosphate (IP3) and diacylglycerol (DAG). The decrease in PIP2 concentration in the immediate vicinity of the channel causes diffusion of bound PIP2 away from the channel-binding site resulting in current inhibition. IP3 stimulates Ca^{2+} release from endoplasmic reticulum stores, while DAG stimulates PKC that phosphorylates many protein targets (Keselman, 2007).

The Gq-coupled GPCR used in this experiment is the 5HT2A serotonin receptor. The 5HT2 receptors are one of seven families that have been identified (5HT1-5HT7) and subpopulations have been described for several of these. The family of 5HT2 receptors are all GPCRs, except for 5HT3 receptors which are nonselective Na^+/K^+ ion channel receptors (Glennon, 2000). The three receptor subtypes within the 5HT2 family have 70 to 80% sequence homology, and have been found to be consistent with those of transmembrane-spanning GPCRs coupled to a phosphoinositol second messenger system (Glennon, 2000). 5HT2A receptors are mainly expressed in the Central Nervous System (CNS), with a distribution of these receptors at

various densities throughout the brain. The highest density is in the neocortex, specifically in the frontal cortex and hippocampus modulating local circuitry. Both of these brain areas are known to be involved importantly in associative learning across a number of species and learning paradigms (Zhang, 2013). These receptors have also received considerable attention from a neuropsychiatric standpoint. Various antipsychotic agents and antidepressants bind with relatively high affinity to the 5HT2A receptors. For example, chronic administration of 5HT2A antagonist results in a paradoxical down-regulation of 5HT2A receptors; such a down- regulation would be of benefit in the treatment of depression (Glennon, 2000). 5HT2A receptors also play a role in anxiety, depression, schizophrenia, migraine and drug abuse. Several 5HT2A antagonists are currently in clinical trails as potential antipsychotic agents. Compared to indolealkylamine and classical hallucinogens (such as LSD), phenylalkylamine hallucinogens (such as DOB, DOI) are much more 5HT2 selective (Glennon, 2002).

Risperidone is an atypical antipsychotic and an inverse agonist at 5HT2A receptors (Marder, 1997). Inverse agonists bind to constitutively active receptors, stabilize them and shift receptor equilibrium towards the inactive state, reducing the level of basal activity (Milligan, 2003). It is most often used to treat delusional psychosis such as schizophrenia, in addition to some forms of bipolar disorder and psychotic depression (Glick, et al, 2001). Schizophrenia is a devastating psychiatric disorder, having its onset in puberty and lasting throughout life (Schotte, 1996). Conventional antipsychotic agents have displayed major shortcomings in the treatment of schizophrenia: the induction of neurological side effects (dystonia, parkinsonism, akathisia, tardive dyskinesia) and often a lack of efficacy for the treatment of the negative symptoms of schizophrenia (Seeman 1980; Ellenbroek 1993). Clinical studies have shown risperidone to improve both the positive symptoms (hallucinations, delusional thinking, severe excitement and

unusual behavior) and the negative symptoms (anergy, apathy, lack of drive, social withdrawal and depressive mood) of schizophrenia with a low incidence of extrapyramidal side effects (EPS) (Megens, 1994). Although both types of symptoms are independent from each other, they may coexist in the same patient (Stevens 1973; Crow 1980; Hafner 1993). It has also shown some success in treating symptoms of Asperger's Syndrome and autism (Fisman, et al, 1996). The actions of risperidone are considered before those of other 5HT2 antagonists because this drug is the most potent and selective 5HT2A antagonist available to clinicians (Schotte, 1996; Richelson and Souder, 2000).

Risperidone is a benzisoxazole derivative. Its molecular structure is shown in Figure 1A. The short-term aim of this study is to examine four deconstructed analogs of risperidone to determine the portion that is important to 5HT2AR functional activity and response. Risperidone was deconstructed by first removing a portion of the diazabicyclo ring to afford RHV-023 and RHV-026 (Fig. 1). The next two compounds, RHV-008 and RHV-006, solely contain the piperidine ring and the benzisoxazole ring system (Fig. 1B). RHV-008 contains a methyl group, derived from the carbon chain, whereas, RHV-006 does not retain the methyl group (Gaitonde, 2013).

We demonstrated that all four deconstructed analogs have a functional effect on the 5HT2A receptor. The data were collected mainly by performing two-electrode voltage clamp recordings and epifluorescence calcium imaging.

Figure 1. Risperidone and its deconstructed analogs along with serotonin.
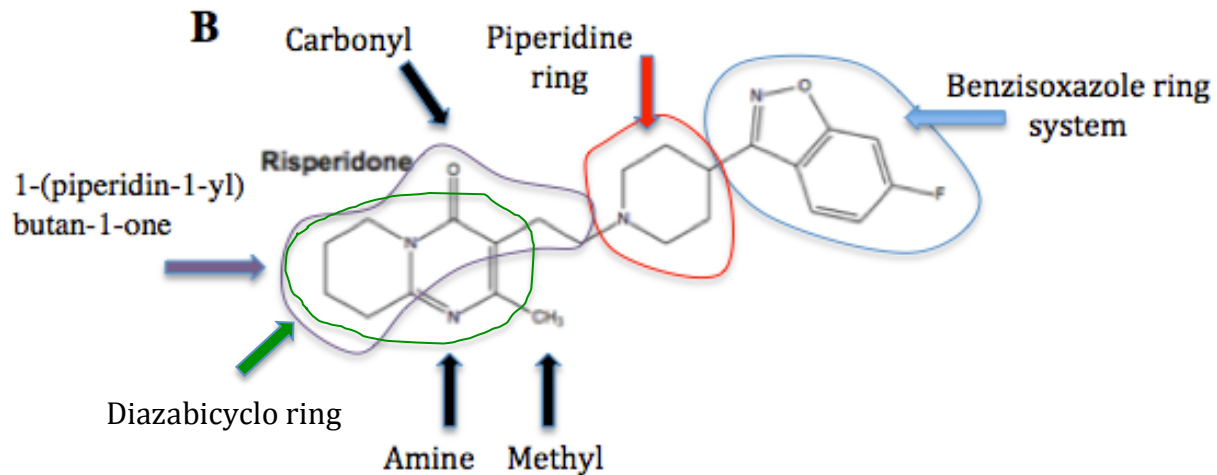
A
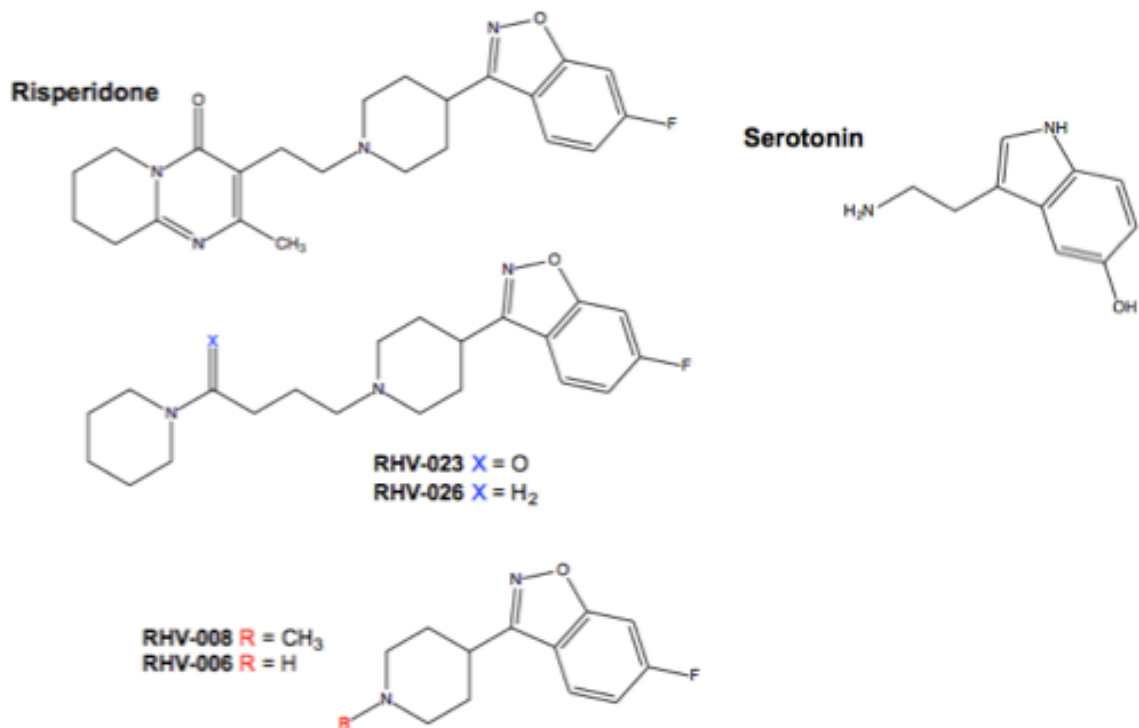
B

Figure 2. PIP2 signaling pathway indirectly modulates ion channels through the activation of protein kinase C (PKC) and Ca²⁺ dependent enzymes using secondary messengers. Activation of phospholipase C (PLC) results in the hydrolysis of phosphatidylinositol (PIP_2) to produce inositol 1,4,5-triphosphate (IP_3) and diacylglycerol (DAG). IP_3 activates Ca^{2+} channels in the endoplasmic reticulum (ER) triggering the release of Ca^{2+} from intracellular stores. The cytoplasmic rise in Ca^{2+} level and DAG then activate protein kinase C (PKC), which in turn phosphorylates K^+ channels, thereby modulating current across the membrane.
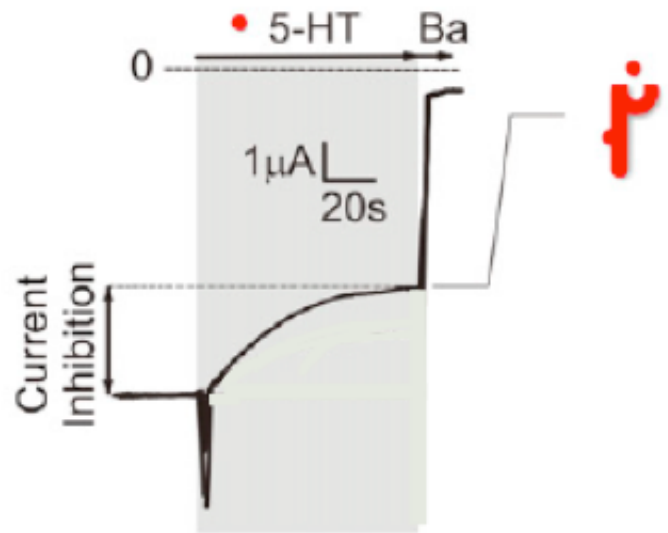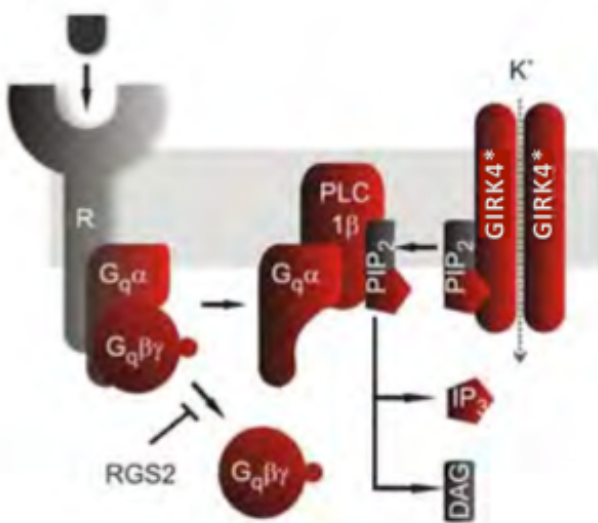
MATERIALS AND METHODS

A) Electrophysiology

Xenopus laevis oocytes have been used as a heterologous expression system for studying ion channels in a controlled cellular environment. Oocytes are enzymatically isolated, and microinjected with 1-2 ng cRNA constructs. Oocytes are then incubated for 2 days at 18°C for expression, as previously described (Solis, et al, 2014). The responses are analyzed electrophysiologically using the two-electrode voltage-clamp technique. A high potassium solution is used to record basal channel expression levels. The high potassium solution contains 96 KCl, 1 NaCl, 1 MgCl2, 5 KOH/HEPES, in mM). A 3mM BaCl2 solution is used to block GIRK4* currents. The presence of an endogenous response is utilized as positive control for the second messenger system coupled to the initial response being studied. In the case of Gq- GPCR, a calcium- induced chloride spike is the endogenous response visualized as a large outward current spike and a smaller inward current spike.

B) HEK-293 cells stably expressing 2AR

This cell line was kindly provided by Dr. Jose Miguel Eltit (Department of Physiology and Biophysics, Virginia Commonwealth University, Richmond, VA). To produce stable inducible cell lines using the Flp-In T- REx expression system (Invitrogen), the 2AR DNA fragment was subcloned into the pcDNA5/FRT/TO vector to generate the pCDNA5/FRT/2AR/FRT/TO plasmid. The inducible expressing cells were made following the manufacturer's protocol. Briefly, the Flp-In T-REx host cell lines are HEK cells with a single FRT recombination site and a Tet repressor gene. The T-Rex system is a tetracycline regulated mammalian expression system that uses regulatory elements. These cells were co- transfected

with the pcDNA5/2AR/FRT/TO and the pOG44 plasmids. The latter encodes the Flp recombinase. Clones that have inserted a single copy of the gene inserted into the recombination site acquire a hdyrogmycin resistance. 2AR was induced adding doxycycline 1ug/mL to the culture media for 3 days.

C) Cell Culture and Transient Transfection

These cells were maintained with guidance by Dr. Lia Baki (Department of Physiology and Biophysics, Virginia Commonwealth University, Richmond, VA). The HEK293 cell line stably expressing 5HT2AR was grown in Dulbecco's modified Eagle's medium (DMEM) (Invitrogen, Carlsbad, CA) supplemented with 10% fetal bovine serum (FBS) (Atlanta Biologicals, Inc., Lawrenceville, GA) and Hygromycin- containing media. The HEK cells were transiently transfected with 5HT2AR.

D) Calcium Imaging

The Ca^{2+} sensitive dye Fura2AM (Life Technologies) was dissolved in DMSO pluronic F-127 20% and then was diluted in Imaging Solution (recipe below). The Ca^{2+} unbound form of Fura2 gets excited at 380 nm and the Ca^{2+} bound form at 340 nm. The emitted light is measured at around 510 nm. The fluorescence intensity increases at 340 nm with increasing Ca^{2+} concentration and decreases at 380 nm for the unbound form resulting in an emitted ratio wavelength of 510 nm. For calcium imaging, load cells with Fura-2 AM (2 μM) diluted in calcium-containing extracellular imaging solution (IS) (130 NaCl, 4 KCl, 2CaCl2, 1MgCl2, 10 Hepes, 10 glucose, pH 7.4, in mM) to get a final concentration of 5.5 μM. The cells were loaded for 25 minutes with Fura-2AM all at 37°C. Fura-2AM is a high affinity, intracellular calcium

indicator that is ratiometric and UV light excitable. Then the cells were washed twice with IS and placed on the stage of an epifluorescence microscope. All the compounds used were dissolved in IS and when high K^+ solution was used in equimolar amount of NaCl it was substituted by KCl. The setup consists of an Olympus IX70 microscope equipped with a polychrome V (Till photonics, Gragelging, Germany) as a light source, a Luca S digital camera (Andor Technology, Belfast, UK), and an automatic perfusion system (AutoMate Scientific, Berkeley, CA). The imaging system was controlled by the Live Acquisition Software from Till Photonics. The measurements were done under constant perfusion at RT (23 degC) or at 35degC using a ThermoClamp-1 heater (AutoMate Scientific, Berkley, CA). The objective used was an Olympus 20x 0.8NA Oil. The Fura-2 signal was acquired switching the excitation wavelength between 340/10nm and 380/10nm at 6Hz, the dichroic mirror used was LP490 and the emission wavelength was 510/40nm. All signals were background subtracted.

E) Statistical Analysis

All oocyte recordings were obtained using Clampfit 9.2 (Molecular Devices, Sunnyvale, CA) and transferred to Excel software (Microsoft, Albuquerque, NM). The first few data points of the current versus time plot were averaged to obtain the basal current. The agonist-induced currents were obtained by averaging several current values that appear immediately after the slope of the ramp current started to change. Similarly, the data points after barium block were averaged. Barium-sensitive basal and agonist-induced currents were calculated by subtracting the current remaining after barium block from basal and agonist-induced currents, determined as described above. In the statistic analysis, basal and agonist-induced currents from each recording were again averaged. Error bars in the figures represent standard error. The standard deviations

for each data set were divided by the square root of the number of recordings to get the standard errors.

All calcium imaging recordings were obtained using Live Acquisition (Innsbruck, Austria) and transferred to Excel software (Microsoft, Albuquerque, NM). The maximum and basal value (average value between 20 and 30 second) was taken. A threshold of 1.05 was used over the ratio of maximum to basal, to distinguish between responsive and non- responsive cells. In statistical analysis, the average maximum values from responsive and non-responsive cells at each concentration of RHV-006/8 were analyzed. Total number of cells was calculated between the two groups. Average time traces were graphed between different concentrations. Error bars in the figures represent standard error. The standard deviations for each data set were divided by the square root of the number of recordings to get the standard errors.

Statistical significance of experiments involving four groups was assessed by one- way ANOVA. Statistical significance of experiments comparing two groups was assessed by Student's t-test.

F) Analogs

The exact chemical names for the deconstructed analogs are as follows: RHV-006 is 6-fluoro-3-(piperidin-4-yl)benzisoxazole, RHV-008 is 6-fluoro-3-(1-methyl-piperidin-4-yl)benzisoxazole,, RHV-023 is 4-[(4-(6-fluorobenzisoxazol-3-yl)piperidin-1-yl)-1-(piperidin-1-yl)]butan-1-one and RHV-026 is 6-fluoro-3-[(1-(4-piperidin-1-yl)butylpiperidin-4-yl)]benzisoxazole. All compounds were submitted as their HCl salts. They were synthesized in the laboratory. The synthesis is represented in the VAS slides and poster (Gaitonde, 2013).

RESULTS

RHV-006 is a partial agonist and suppresses 5-HT activity on the 5HT2A receptor.

Figure 3 shows time course examples of serotonin and RHV-006 effects on GIRK currents. Figure 3A reports currents at Vm=-80mV (negative currents) and Vm=+80mV (positive currents). 1µM 5-HT elicited large transient calcium-activated chloride currents that showed outward rectification. In addition, there is a 5-HT induced inhibition of the inwardly rectifying GIRK4* current. In contrast, RHV-006 did not induce calcium-activated chloride current spikes, but did inhibit GIRK4* currents (Figure 3B). When comparing the relative inhibition by these ligands, 5-HT at 1μM and RHV-006 at 10 µM, the risperidone fragment elicited 34% agonism compared to 5-HT from 10 experiments in oocytes from 3 different frogs (Figure 4). The RHV-006 effects showed saturation by 0.1μM (Figure 5). Additional experiments will be necessary to obtain a full dose-response leading to the saturated levels of the effect. When applied together with 1μM 5-HT, 10 μM RHV-006 reduced G_q activity by ~67% (Figure 6), bringing the current to its saturated level of partial agonism (see Figure 6). A dose-dependent response of RHV-006 inhibition of the 5-HT response is shown in Figure 7, where it can be seen that the half maximal inhibition lies between 0.1-5 µM.

RHV-008 is also a partial agonist and suppresses 5-HT activity on the 5HT2A receptor.

Figure 8 shows current time courses for 5-HT (Figure 8A) and RHV-008 (Figure 8B). Just like, RHV-006, RHV-008 did not induce Ca^{2+}-activated Cl^- currents. RHV-008 elicited 27% agonism when applied alone at 10µM (Figure 9). Application of RHV-008 alone showed partial agonism saturation by 10µM (Figure 10). Additional experiments will be required for a full dose-response curve to determine the EC_{50} value for this compound. When applied together with 1μM 5-HT, 10

μM RHV-008 reduced G_q activity by ~77% (Figure 11). Application of RHV-008 together with 1 μM 5-HT showed that the receptors became saturated by around 5 μM (Figure 12).

RHV-023 and RHV-026 are weak agonists and have an additive effect on 5-HT activity on 5HT2AR.

Application of 10μM RHV-023 and RHV-026 together with 1μM 5-HT produced partial agonism of ~45% and ~74%, respectively (Figure 13) (data produced by Jason Younkin and Peter Drossopoulos)). Figure 13 compares the partial agonism of all four deconstructed risperidone fragments. In the presence of 5-HT, RHV-023 and RHV-026 did not decrease the 5-HT-mediated inhibition of K^+ currents (Figure 14). In fact, RHV-026 was additive to the 5-HT effect, suggesting that these two compounds did not compete with 5-HT to trigger their effects.

Figure 15 summarizes the effects of the deconstructed risperidone fragments on their partial agonism and their effect on the 5-HT effects on the 5HT2AR.

Cells transfected with 2AR show a decrease in calcium signaling when RHV-006 or RHV-008 is added along with 5-HT.

The addition of 1μM 5-HT to 2AR expressing HEK-293 cells using epifluorescence showed a robust calcium signaling increase, with the Fura2 ratio (340/380nm) reaching 1.6 (Figure 16A). However, addition of 10 μM of RHV-006 (Figure 16D) or RHV-008 (Figure 16E) alone did not elicit a calcium signal, consistent with the experiments in oocytes where these compounds did not elicit Ca^{2+}-activated Cl^- currents (see Figures 3B and 8B). When 10μM of RHV-006 (Figure 16B) or RHV-008 (Figure 16C) was added to 2AR cells in the presence of 1μM 5-HT, however,

both the number of cells responding and the level of responses to 5-HT decreased. Only 28% of all cells showed a calcium response to 10μM RHV-006 in the presence of 1μM 5-HT. 30% of all cells showed a calcium response to 10μM RHV-008 in the presence of 1μM 5-HT (Figure 17). Thus, a large number of cells did not show a calcium response to 1μM 5-HT in the presence of 10μM RHV-006/8. Furthermore, the level of response of the responsive cells decreased with the addition of RHV-006/8. Addition of 10μM RHV-006 showed an approximately 65% decrease in the Fura2 ratio calcium response (Figures 16B, 18) compared to that of 1μM 5-HT. Addition of 10μM RHV-008 showed an approximately 40% decrease in the Fura2 ratio calcium response (Figures 16C, 18) compared to that of 1μM 5-HT. A dose response, using the addition of 7 concentrations of RHV-008 (0.01uM, 0.1μM, 0.5uM, 1μM, 5uM, 10μM, 100uM) to 1μM 5-HT, showed a decrease of the level of response (Figures 19, 20) starting at 5 μM RHV-008. 100 μM RHV-008 and 1 μM 5-HT showed almost no calcium response – the signal was completely quenched at this concentration. Interestingly, the concentrations lower than 5uM showed a kinetic change, according to their decrease in Fura2 ratio level of response over a period of time compared to the time trace of 1μM 5-HT applied alone.

Figure 3. Gq signaling activity of 2AR in response to serotonin and

RHV-006. Representative barium- sensitive traces of GIRK4* currents obtained in oocytes in (A) response to 1μM serotonin (5-HT) and (B) response to 10 μM of RHV-006. Note the lack of a calcium- induced chloride spike, visualized as a large spike in the outward current, when RHV-006 is added, compared to an evident spike with serotonin.
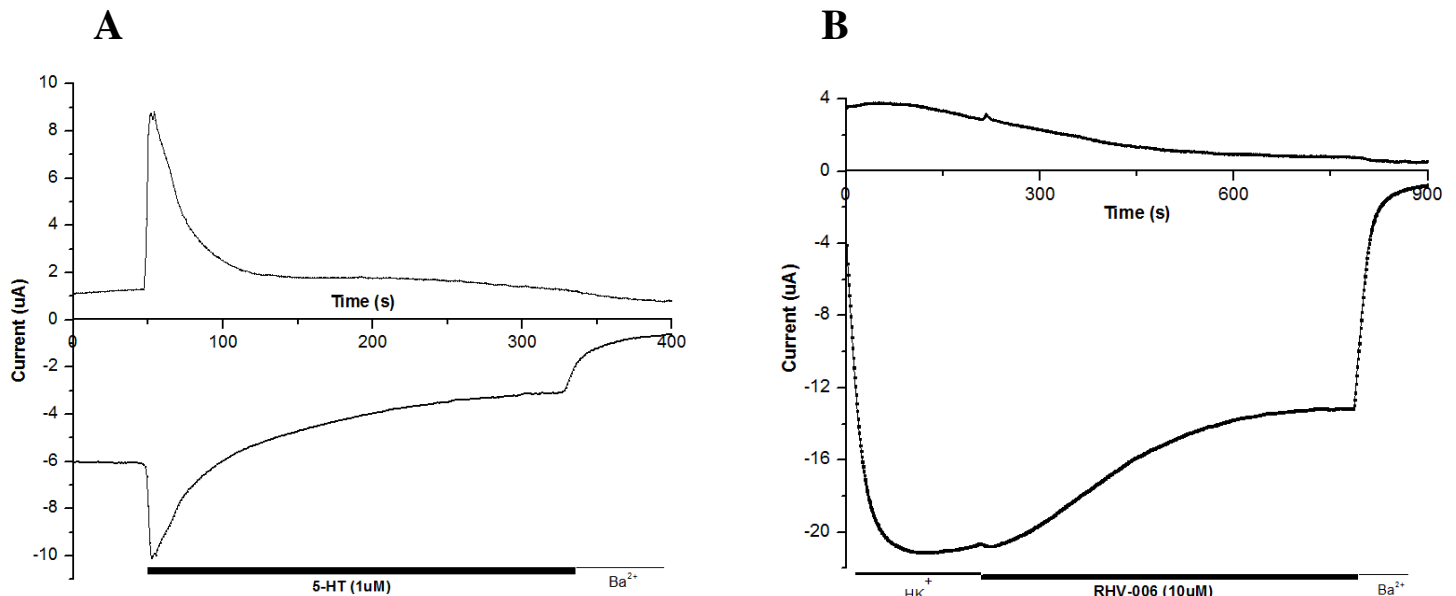
Figure 4. Agonism of 10μM RHV-006 on 2AR. Normalized Gq activity

(GIRK4* current inhibition) compared to basal currents of 10μM RHV-006 obtained in oocytes

expressing 2AR. Each bar is normalized to the Gq activity of 1μM 5-HT. Each bar represents

n=3 frogs and 10 oocytes each with error bars depicting the standard error of the mean.

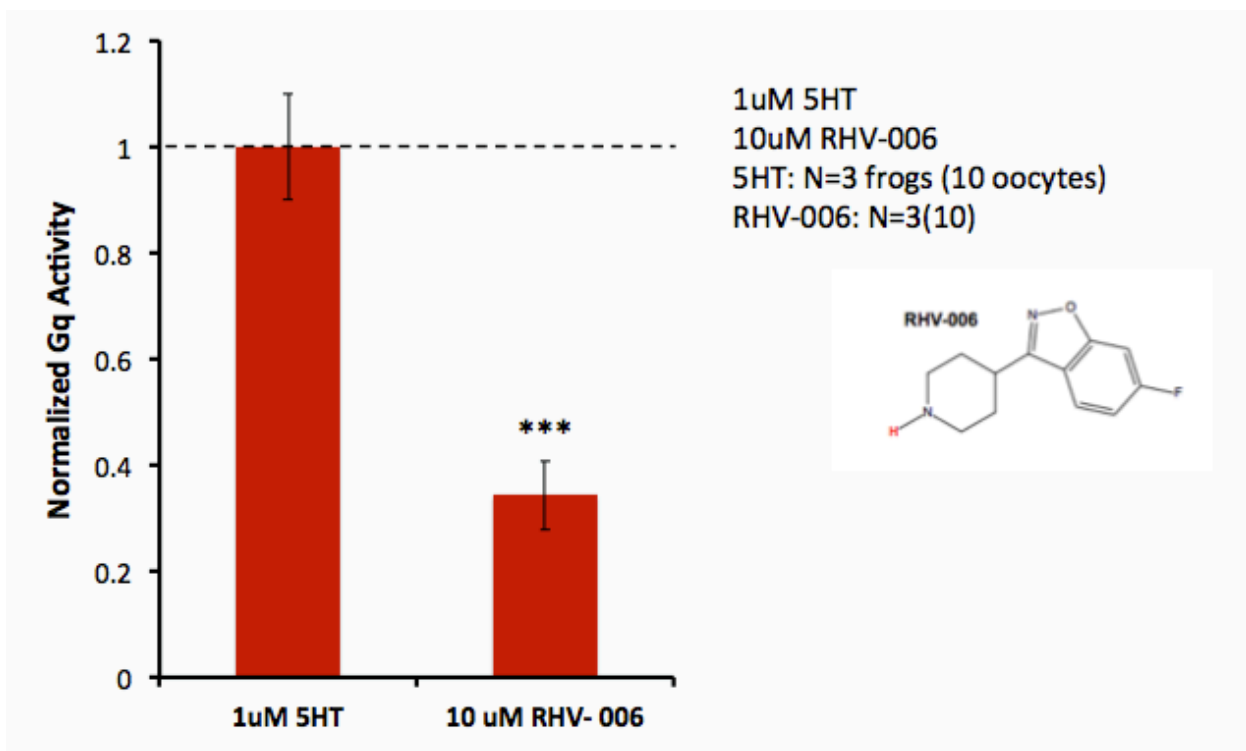(*** indicates 95% confidence intervals do not overlap; estimated p-value ≤ 0.001 compared to

1μM 5-HT)

Figure 5. Saturation of RHV-006 Agonism. Summary of normalized Gq

activity (GIRK4* current inhibition) compared to basal currents obtained in oocytes expressing

2AR in response to increasing concentrations (0.01uM to 10µM) of RHV-006. By 0.1µM RHV-

006, saturating agonist effects have been reached; 10µM of RHV-006 does not give any larger

effect. Each bar is normalized to the Gq activity of 1µM 5-HT. Each bar represents n=1 frog and

4-5 oocytes each with error bars depicting the standard error of the mean. (*** indicates

p<0.0001 for comparison to 1µM 5-HT. # indicates p<0.05 for comparison to 0.01µM RHV-
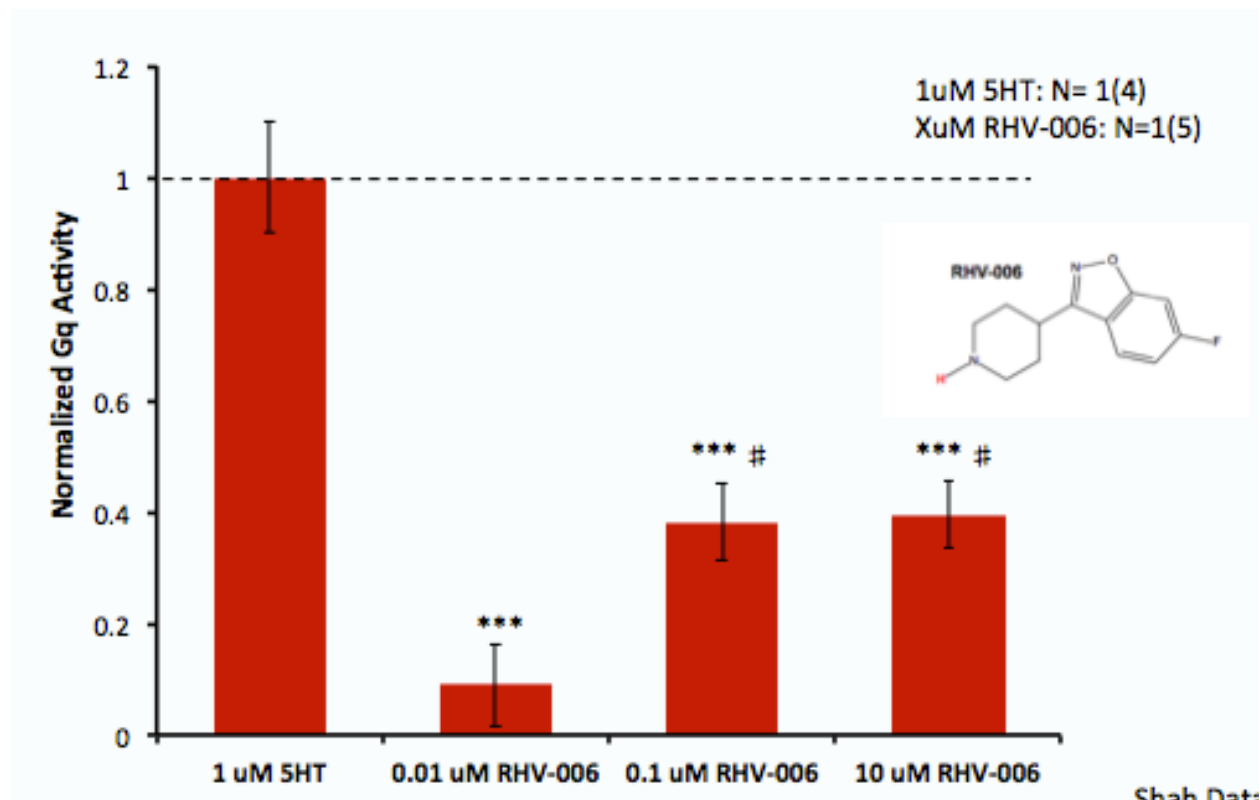
006)

Figure 6. Effect of 10μM RHV-006 in the presence of 5-HT on 5HT2AR. Normalized Gq activity (GIRK4* current inhibition) compared to basal currents of 10μM RHV-006 in the presence of 1μM 5-HT obtained in oocytes expressing 2AR. Each bar is normalized to the Gq activity of 1μM 5-HT. Each bar represents n=3 frogs and 15 oocytes each with error bars depicting the standard error of the mean. (*** indicates 95% confidence intervals do not overlap; estimated p-value ≤ 0.001 compared to 1μM 5-HT)

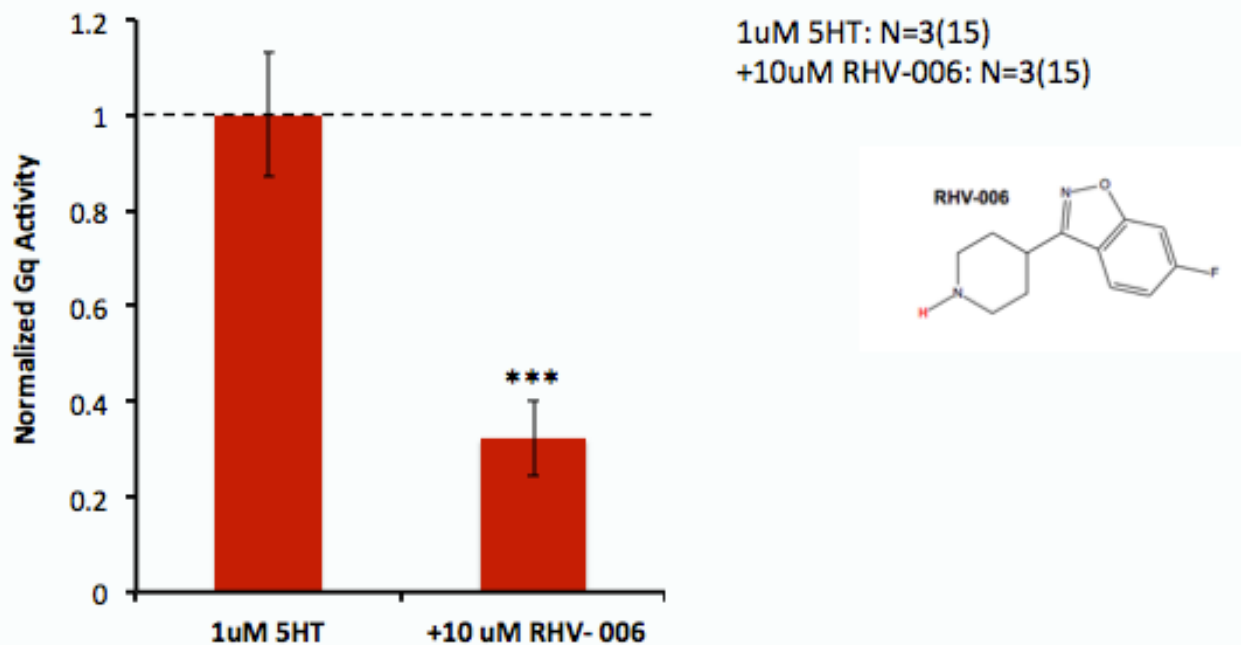**Figure 7. Inhibition Dose Response of RHV-006 in the presence of 5-HT.** Summary of normalized Gq activity (GIRK4* current inhibition) compared to basal currents obtained in oocytes expressing 2AR in response to increasing concentrations (0.01uM to 10μM) of RHV-006 in the presence of 1μM 5-HT. Each bar is normalized to the Gq activity of 1μM 5-HT. (*** indicates $p < 0.0001$ for comparison to 1μM 5-HT. ♯♯♯ indicates $p < 0.0001$ for comparison to 1μM 5-HT + 0.01μM RHV-006)
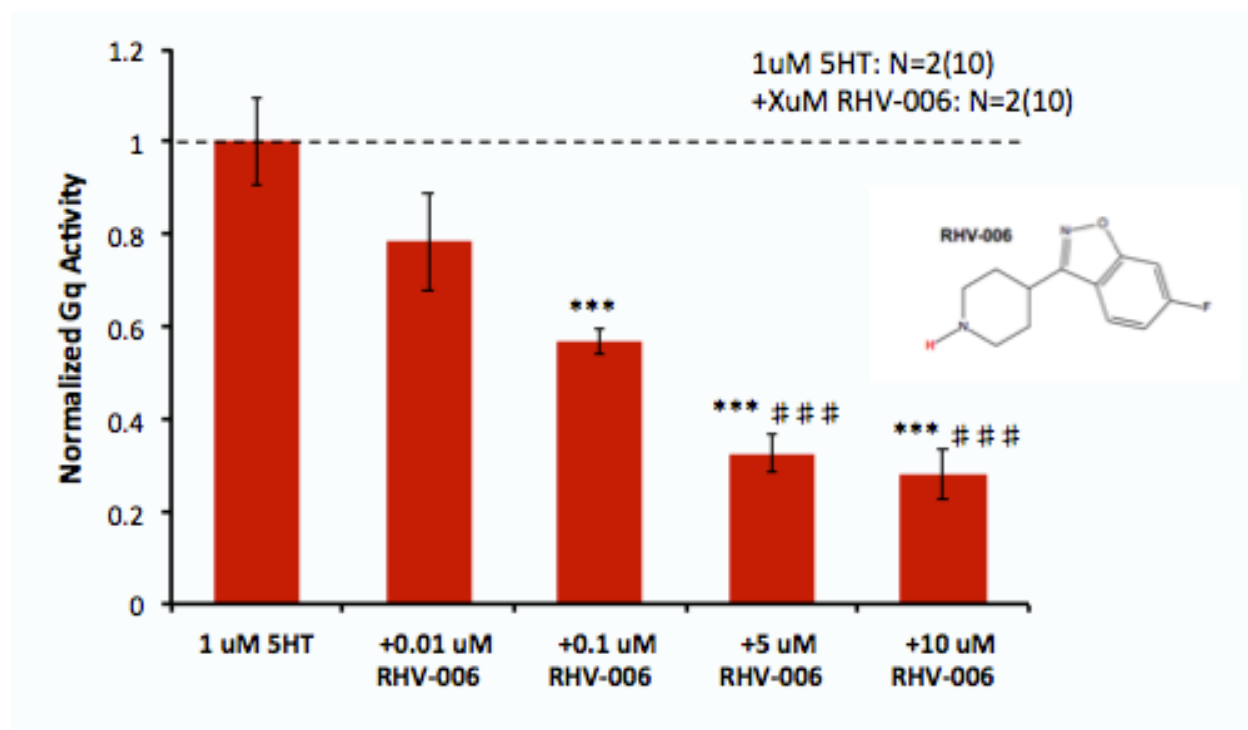
Figure 8. Gq signaling activity of 2AR in response to serotonin and

RHV-008. Representative barium- sensitive traces of GIRK4* currents obtained in oocytes in (A) response to 1μM serotonin (5-HT) and (B) response to 10 μM of RHV-008. Note the lack of a calcium- induced chloride spike, visualized as a large spike in the outward current, when RHV-006 is added, compared to an evident spike with serotonin.
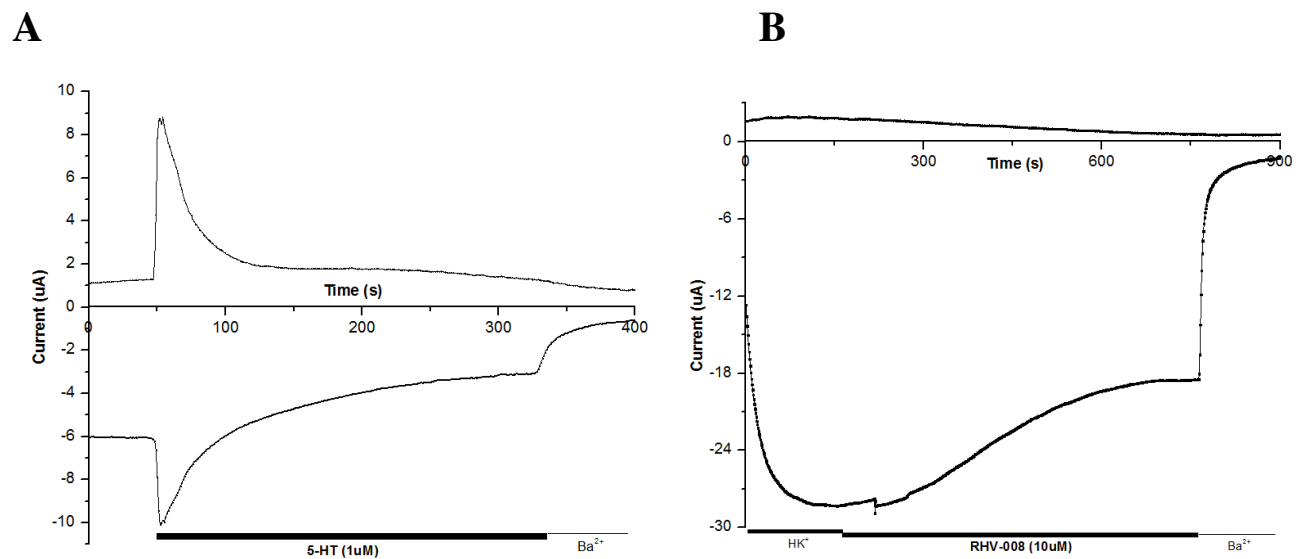
A

B

Figure 9. Agonism of 10μM RHV-008 on 5HT2AR. Normalized Gq activity

(GIRK4* current inhibition) compared to basal currents of 10μM RHV-008 obtained in oocytes

expressing 2AR. Each bar is normalized to the Gq activity of 1μM 5-HT. Each bar represents

n=3 frogs and 12 oocytes each with error bars depicting the standard error of the mean. (***

indicates 95% confidence intervals do not overlap; estimated p-value $\leq$ 0.001 compared to 1μM
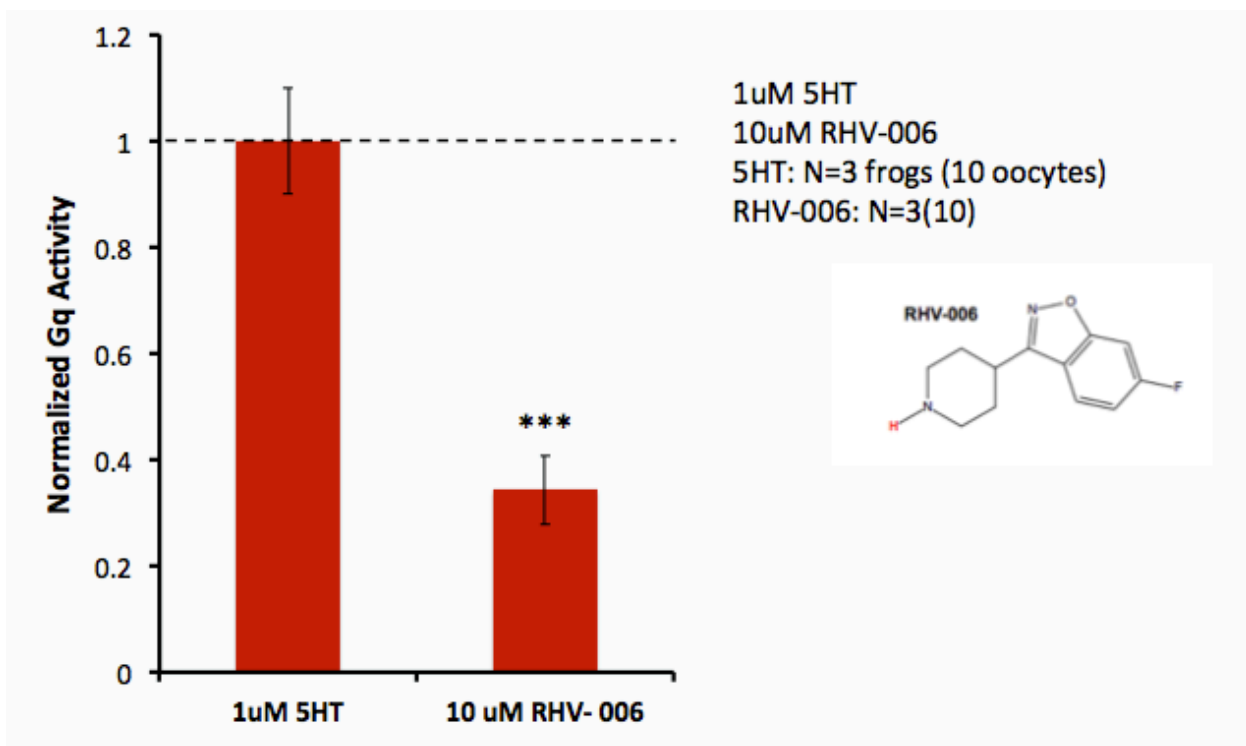
5-HT)

Figure 10. Saturation of RHV-008 Agonism. Summary normalized Gq activity

(GIRK4* current inhibition) compared to basal currents obtained in oocytes expressing 2AR in

response to increasing concentrations (0.1μM to 100uM) of RHV-008. By 10μM RHV-008,

saturating agonist effects have been reached; 100uM of RHV-006 does not give any larger effect.

Each bar is normalized to the Gq activity of 1μM 5-HT. (* indicates 95% confidence intervals do
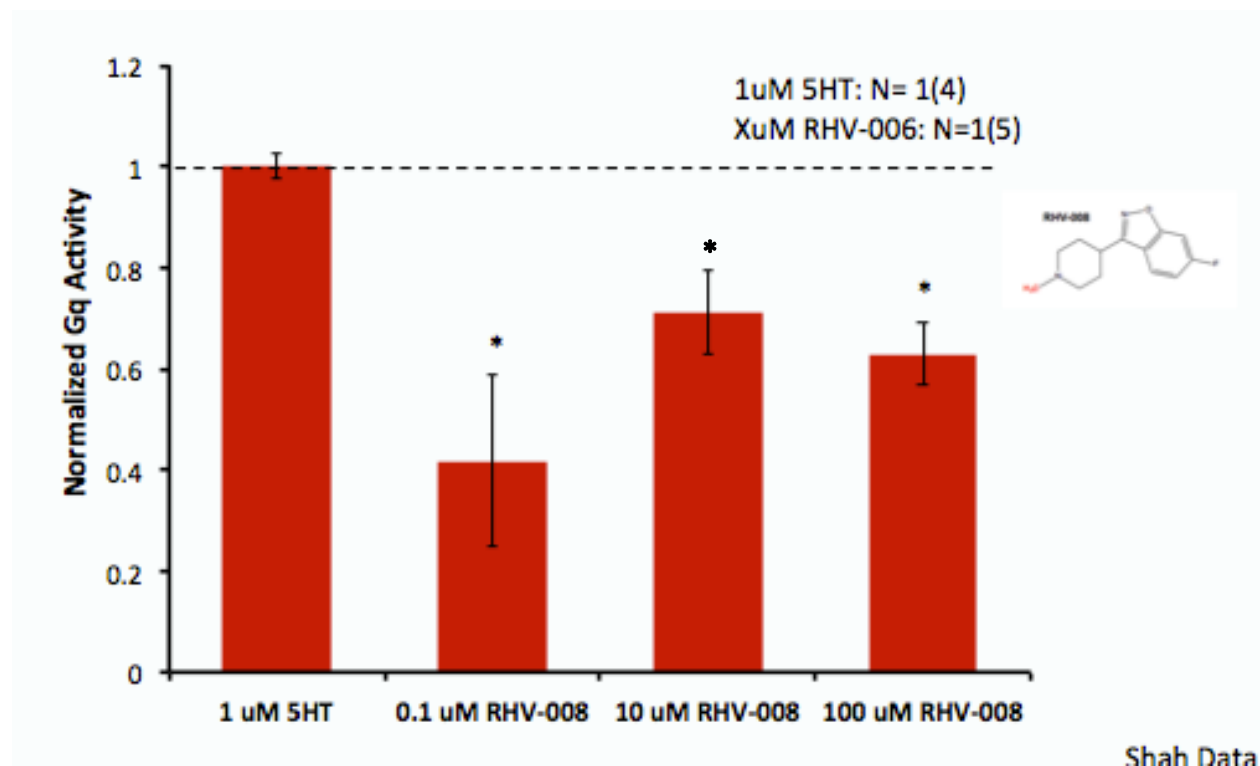
not overlap; estimated p-value<0.05 compared to 1μM 5-HT)

Figure 11. Effect of 10μM RHV-008 in the presence of 5-HT on

5HT2AR. Normalized Gq activity (GIRK4* current inhibition) compared to basal currents of 10μM RHV-008 in the presence of 1μM 5-HT obtained in oocytes expressing 2AR. Each bar is normalized to the Gq activity of 1μM 5-HT. Each bar represents n=3 frogs and 12 oocytes each with error bars depicting the standard error of the mean. (*** indicates 95% confidence intervals do not overlap; estimated p-value ≤ 0.001 compared to 1μM 5-HT)
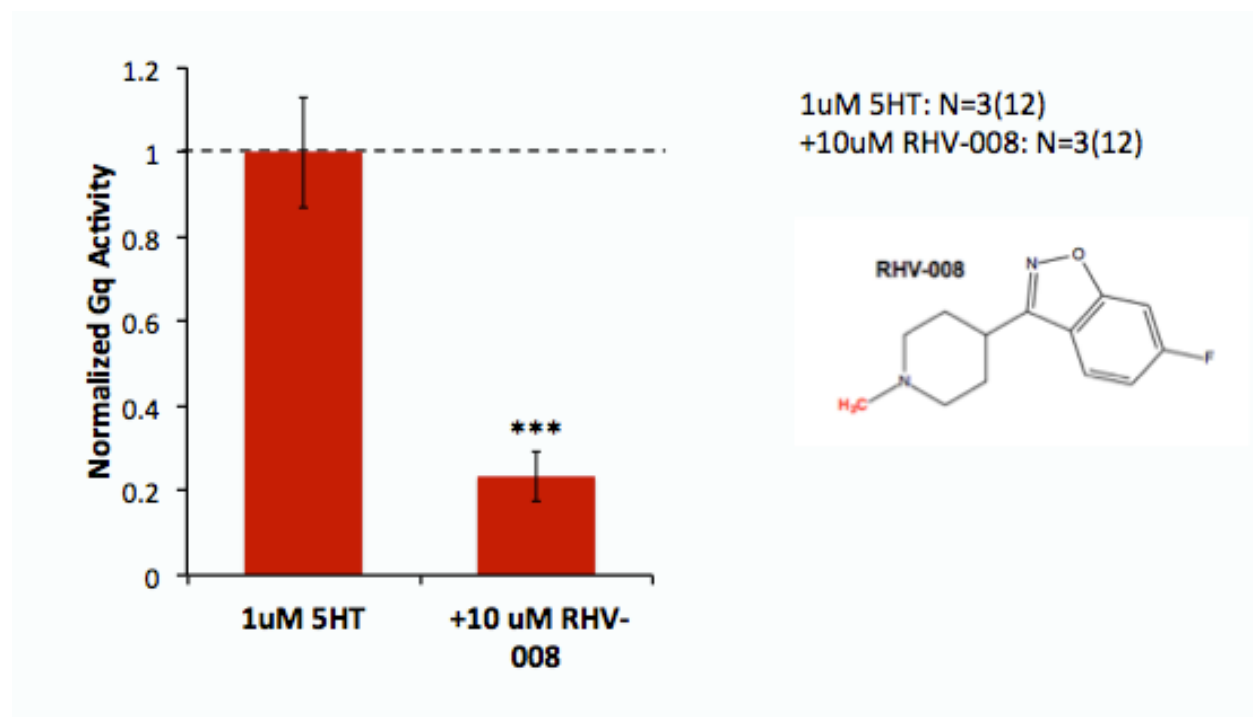
Figure 12. Inhibition Dose Response of RHV-008 in the presence of

5-HT. Summary of normalized Gq activity (GIRK4* current inhibition) compared to basal

currents obtained in oocytes expressing 2AR in response to increasing concentrations (0.1µM to

10µM) of RHV-008 in the presence of 1µM 5-HT. Each bar is normalized to the Gq activity of

1µM 5-HT. (*** indicates p<0.0001 for comparison to 1µM 5-HT. ＃＃＃ indicates p<0.0001

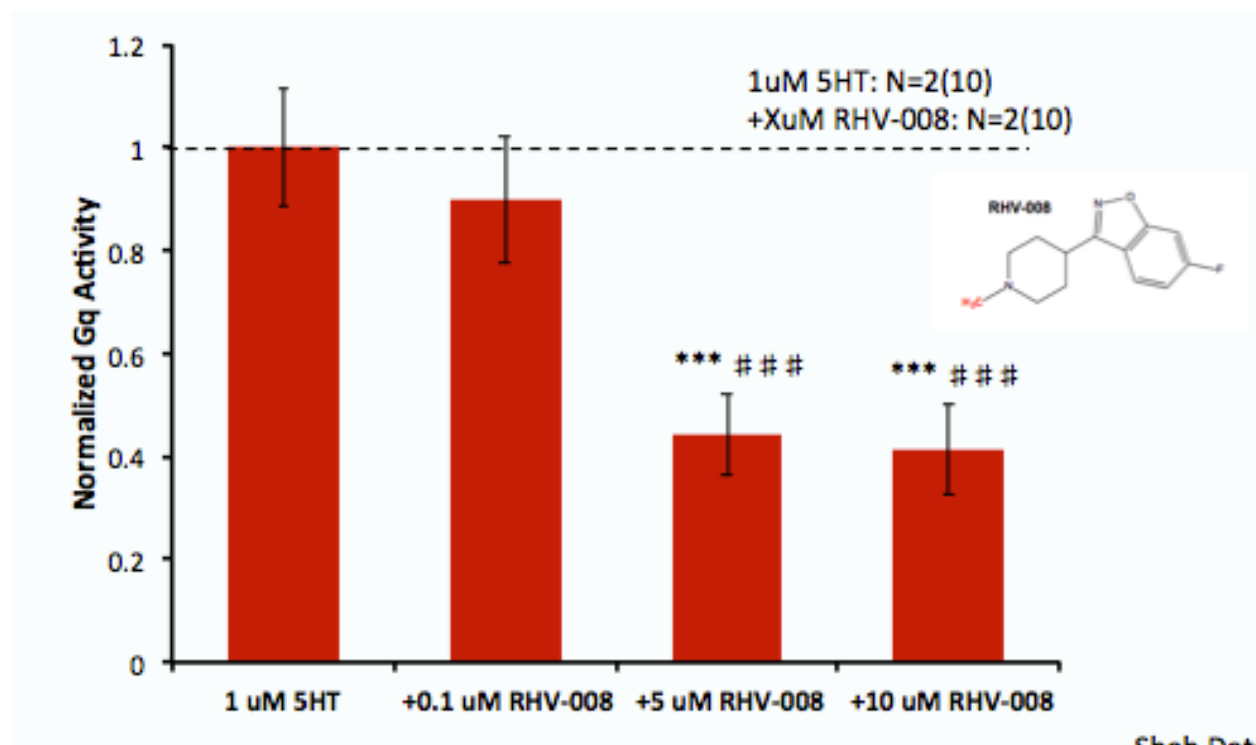for comparison to 1µM 5-HT + 0.1µM RHV-008)

Figure 13. RHV Agonism Totals. Summary bar graph of the agonist- induced Gq

activity of RHV-006, RHV-008, RHV-023 and RHV-026. Each bar is normalized to the Gq

activity of 1μM 5-HT. Each bar represents n=2-3 frogs and 7-12 oocytes each with error bars

depicting the standard error of the mean. (*** indicates p<0.0001 for comparison to 1μM 5-HT.

＃＃ indicates p<0.001 for comparison to 10μM RHV-008, **$** indicates p<0.0.05 for
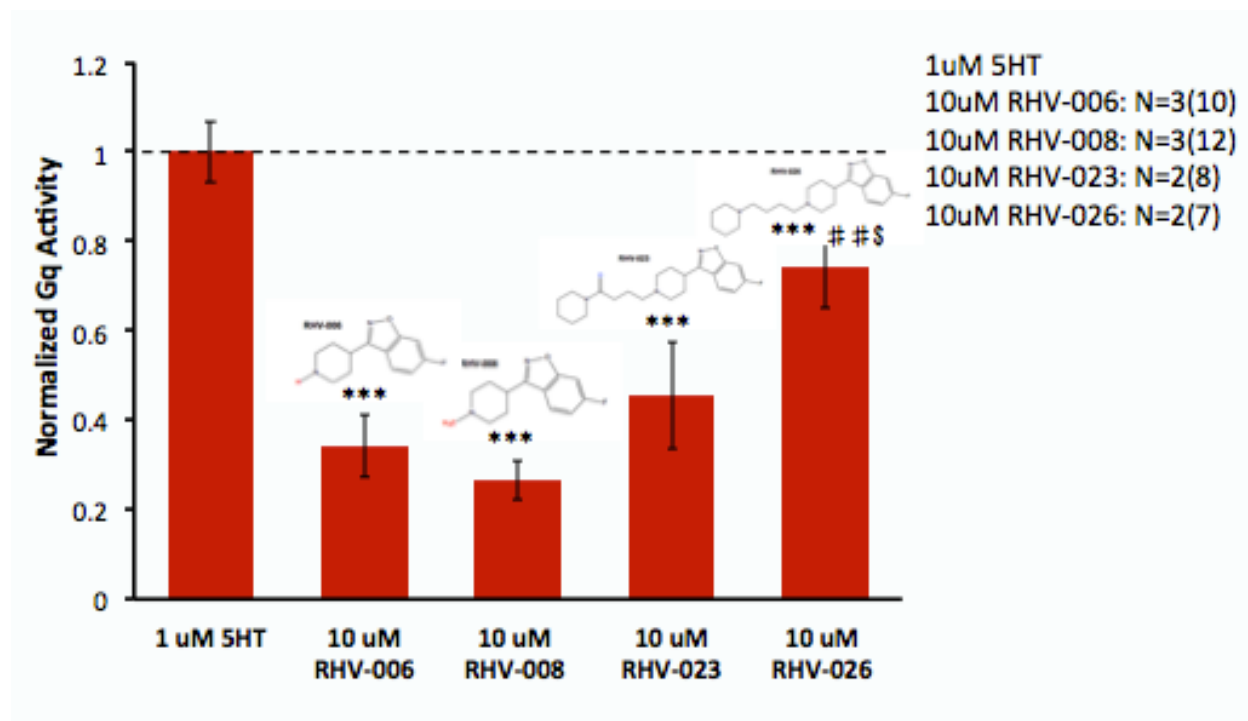
comparison to 10μM RHV-006)

Figure 14. Total RHV Effects in the Presence of 5-HT. Summary bar graph of the agonist- induced Gq activity in the presence of 1μM 5-HT of RHV-006, RHV-008, RHV-023 and RHV-026. Each bar is normalized to the Gq activity of 1μM 5-HT. Each bar represents n=3 frogs and 12-15 oocytes each with error bars depicting the standard error of the mean. (*** indicates $p < 0.0001$ for comparison to 1μM 5-HT, ** indicates $p < 0.001$ for comparison to 1μM 5-HT, * indicates $p < 0.05$ for comparison to 1μM 5-HT. ♯♯♯ indicates $p < 0.0001$ for comparison to 10μM RHV-006 and 10μM RHV-008, $ indicates $p < 0.05$ for comparison to 10μM RHV-023)

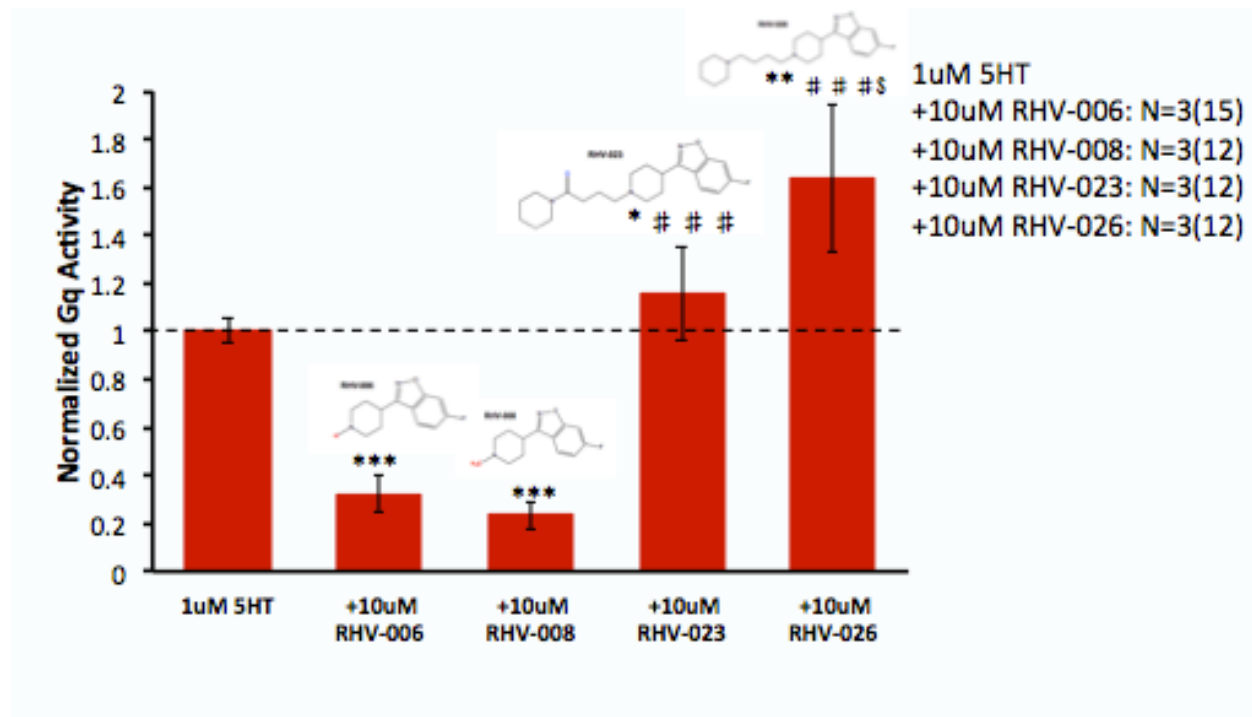**Figure 15. Summary of RHV Analogs.** Summary chart of the agonist-induced Gq

activity values of RHV-006, RHV-008, RHV-023 and RHV-026 compared to 1μM 5-HT (100%

Gq activity).

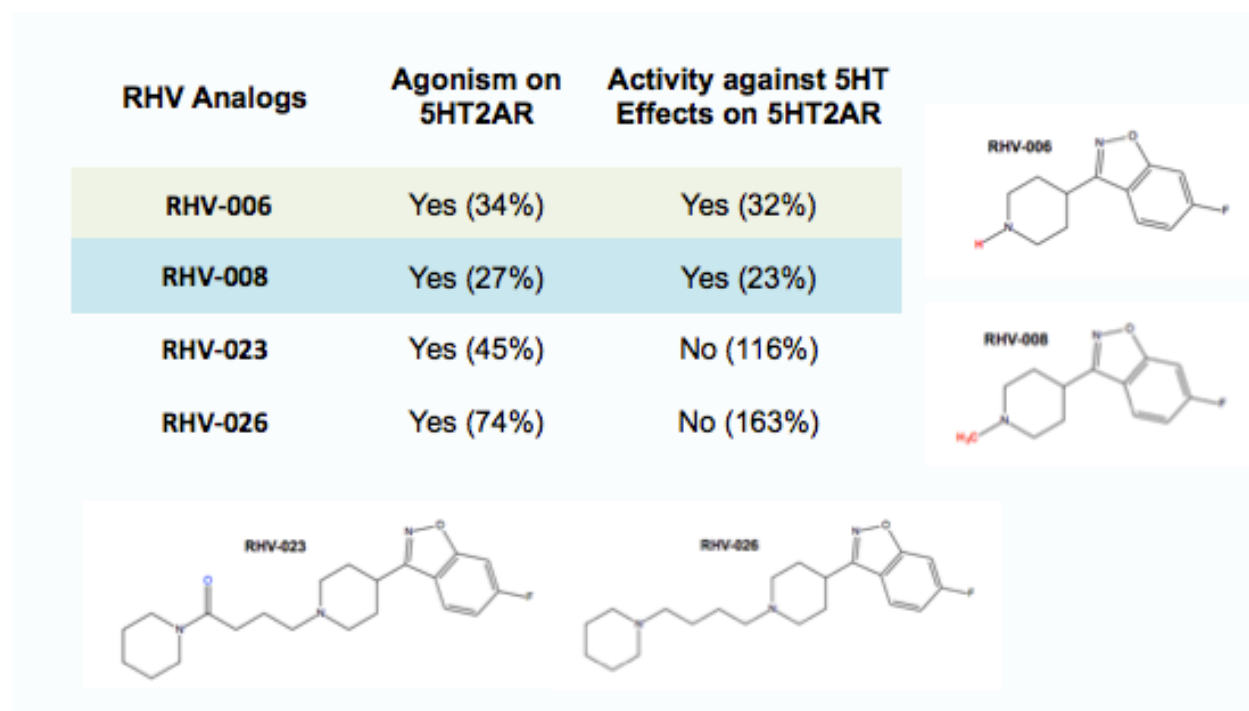| RHV Analogs	Agonism on 5HT2AR	Activity against 5HT Effects on 5HT2AR
RHV-006	Yes (34%)	Yes (32%)
RHV-008	Yes (27%)	Yes (23%)
RHV-023	Yes (45%)	No (116%)
RHV-026	Yes (74%)	No (163%)

Figure 16. Calcium Signal of RHV-006 and RHV-008 by themselves and in the Presence of 5-HT using Epifluorescence Assay. Three images of representative time series of Fura2 fluoresence intensity (340nm/380nm) obtained in HEK cells expressing 2AR with the addition at 30 seconds of (A) 1μM Serotonin, (B) 1μM Serotonin and 10μM RHV-006, (C) 1μM serotonin and 10μM RHV-008. The protocol for (A), (B) and (C) is: low potassium (30 s), compounds (45 s) and low potassium (30 s). Two images of representative time series of Fura2 fluoresence intensity (340nm/380nm) obtained in HEK cells expressing 2AR with the addition at 30 seconds of (D) 10μM RHV-006 and (E) 10μM RHV-008 shows no calcium response; after washing with low potassium, 1μM of serotonin is added at 85 seconds in (D) and (E). The protocol for (D) and (E) is: low potassium (30 s), compound (45 s), 1μM serotonin (30 s), low potassium (30 s). Each line depicts one cell.
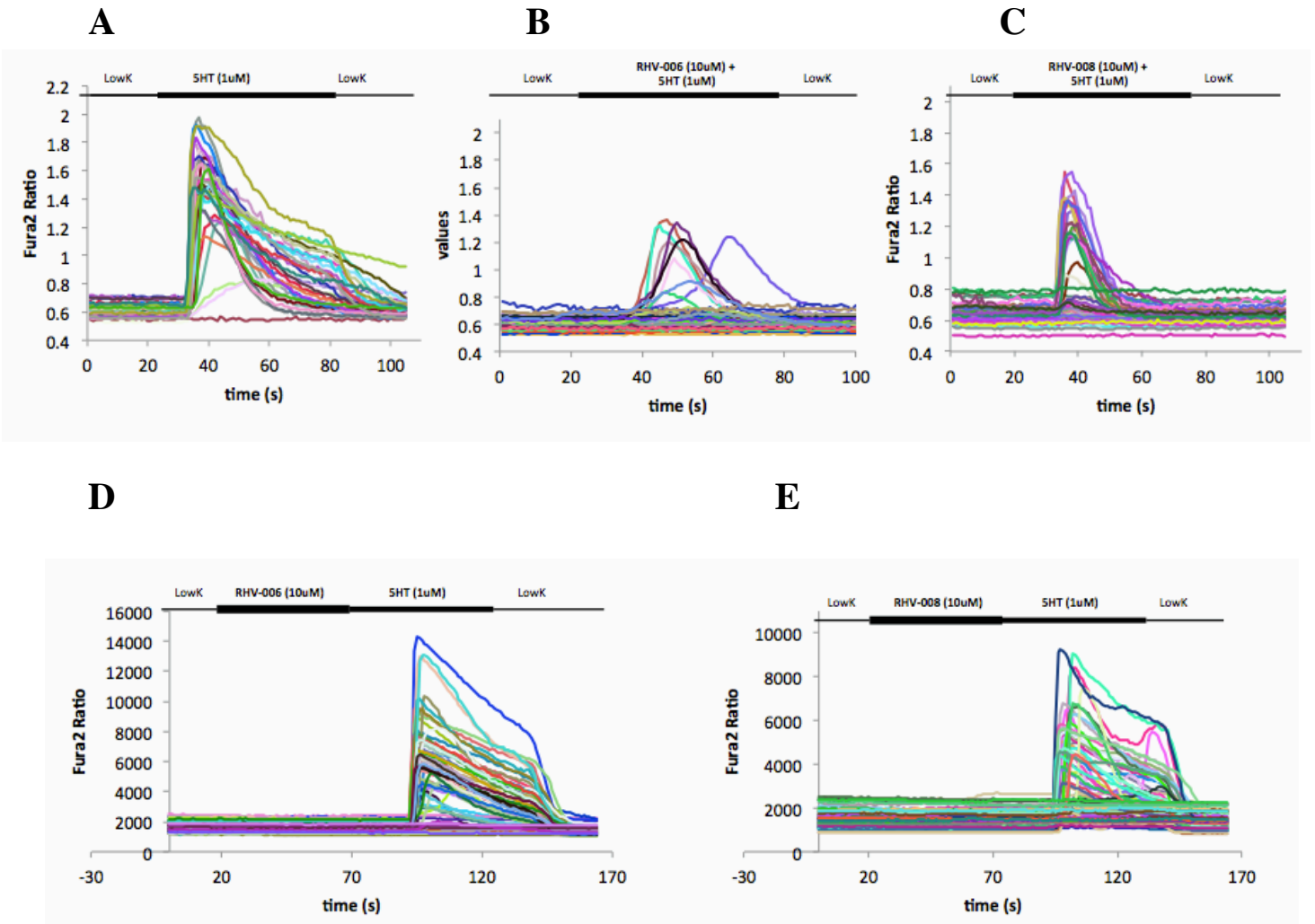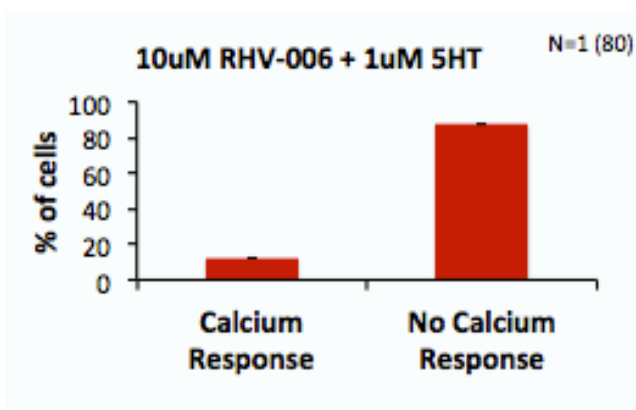
Figure 17. % Calcium Responsive Cells vs % Non- Calcium Responsive Cells of RHV-006 and RHV-008 in the presence of 5-HT.

The bar graph summarizes the percent of calicium responsive and non- calcium responsive cells of (A) 10μM RHV-006 in the presence of 1μM 5-HT (1 experiment in 80 cells total) and (B)10μM RHV-008 in the presence of 1μM 5-HT (1 experiment in 94 cells total). (C) shows a summary chart of percent values of calcium responsive and non- calcium responsive cells of both RHV-006 and RHV-008 in the presence of 1μM 5-HT.

A

B
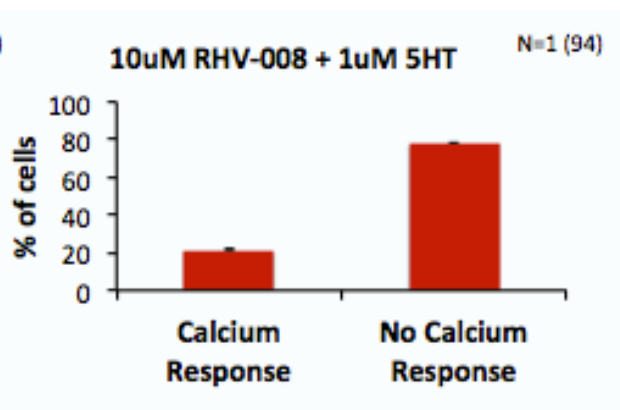
C

	Calcium Response	No Calcium Response
10uM RHV-006 + 1uM 5HT	12%	88%
10um RHV-008 + 1uM 5HT	22%	78%

Figure 18. Normalized Calcium Response of Responsive Cells of RHV-006 and RHV-008 in the presence of 5-HT. Fura2 fluoresence maximal intensities of 1μM 5-HT, the addition of 10μM RHV-006 and 10μM RHV-008 were evaluated at 30 seconds and normalized to their initial values at 0 seconds (100%). All ratios were then normalized to the ratio of 1μM 5-HT. The protocol is low potassium (30 s), compounds (45 s) and low potassium (30 s). Only HEK293 cells showing a calcium response were analyzed. (*** indicates 95% confidence intervals do not overlap; estimated p-value ≤ 0.001 compared to 1μM 5-HT)
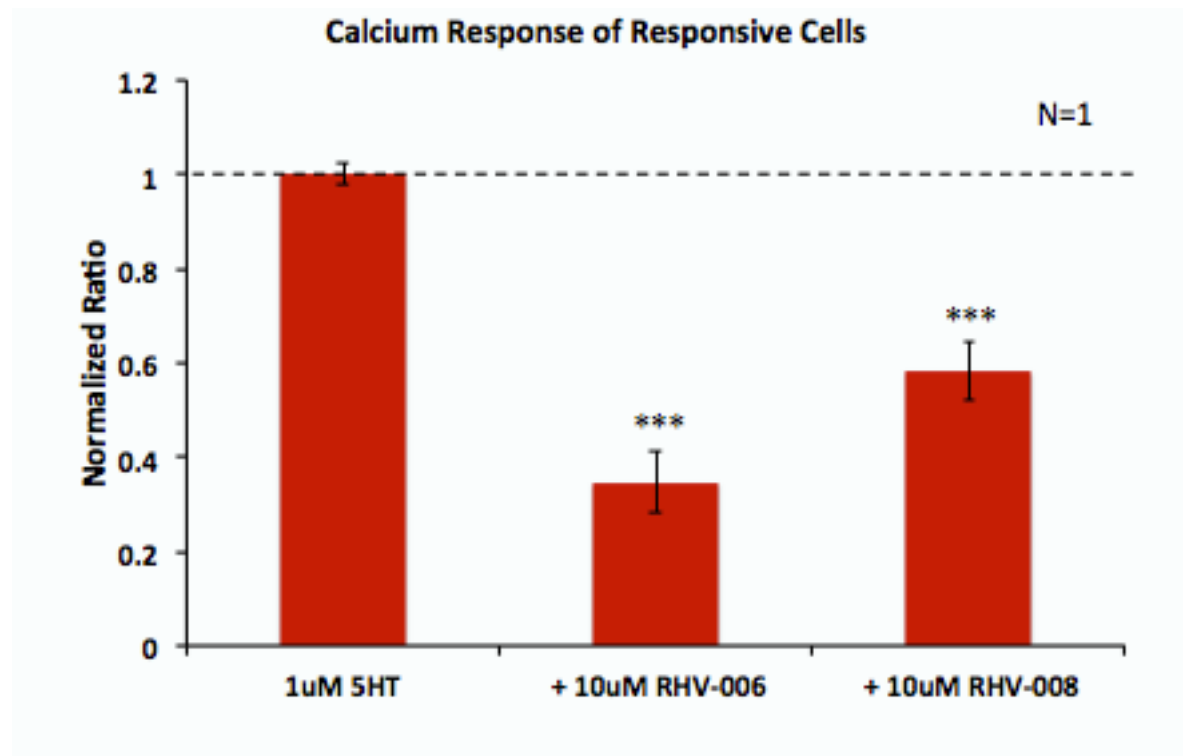
Figure 19. Average Time Traces of Responsive Cells of RHV-008 at Various Concentrations in the Presence of 1μM 5-HT. Representative time series of Fura2 fluoresence intensity (340nm/380nm) obtained in HEK cells expressing 2AR with the addition at 30 seconds of increasing concentrations (0.01uM to 100uM) of RHV-008 in the presence of 1μM 5-HT. The protocol is low potassium (30 s), compounds (45 s) and low potassium (30 s). Only HEK293 cells showing a calcium response were analyzed.
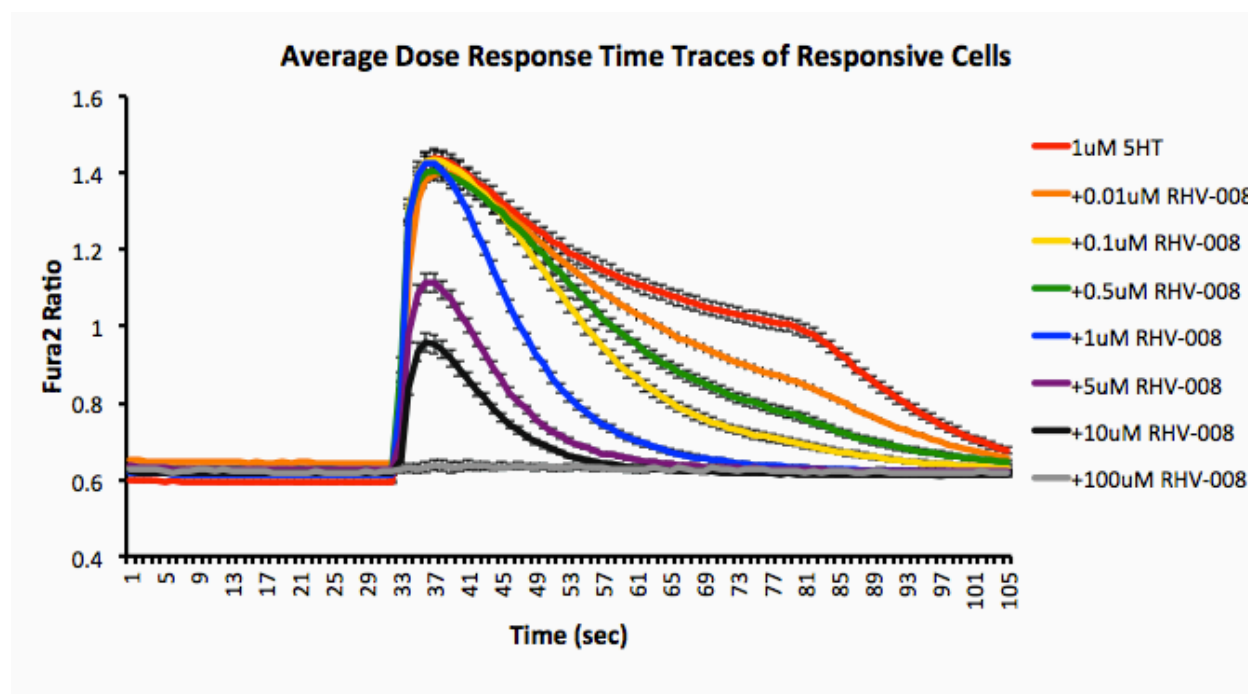
Figure 20. Inhibition Dose Response of RHV-008 in the presence of

5-HT in HEK Cells. Fura2 fluoresence intensities of 1μM 5-HT and the addition of

increasing concentrations (0.01uM to 100uM) of RHV-008 were evaluated at 30 seconds and

normalized to their initial values at 0 seconds (100%). All ratios were then normalized to the

ratio of 1μM 5-HT. The protocol was as follows: 30 seconds of low potassium solution, 45

seconds of solution of interest and 30 seconds of low potassium solution. Only HEK293 cells

showing a calcium response were analyzed.
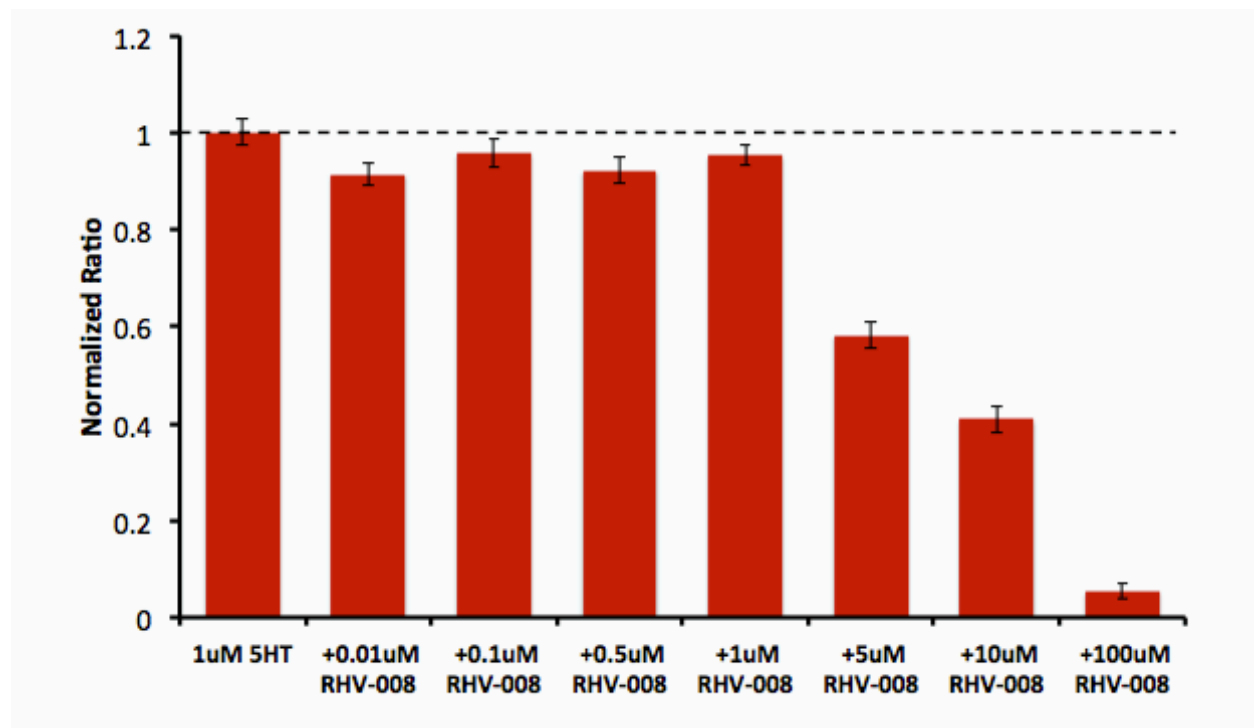
DISCUSSION AND FUTURE DIRECTIONS

The purpose of this study was to examine four deconstructed analogs of risperidone to determine the portion(s) of the molecule that is (are) important to 5HT2AR functional activity and response (Figure 1). Risperidone is a novel antipsychotic that possesses advantages over other antipsychotic agents in terms of efficacy and side effects. Ascertaining which analog accounts for risperidone's action was investigated in two functional assays: the two-electrode-voltage clamp (TEVC) and the Epifluorescence technique. We employed the GIRK4* channel as a reporter of Gq-coupled GPCR signaling and used two-electrode voltage-clamp to monitor currents. Perfusion with $1\mu M$ 5-HT caused a robust inhibition of K^+ current. The spike observed at the onset of serotonin perfusion signifies activation of the oocyte endogenous Ca^{2+}- activated chloride current (I_{Cl-Ca}) and provides additional evidence of the serotonin- induced PIP2 hydrolysis and IP3 mediated rise in intracellular Ca^{2+} (Figure 2).

The normalized Gq activation (relative to the maximal current inhibition – 100%) was plotted as a function of serotonin concentration. Perfusion with $10\mu M$ RHV-006 (Figure 4) or RHV-008 (Figure 9) alone showed approximately 30% normalized Gq activity using a TEVC functional assay. Although inhibition of current was clear, we did not observe a Ca^{2+}-activated chloride current spike. In the TEVC assay, these deconstructed analogs were seen as partial agonists. Interestingly, neither compound elicited a calcium signal while using Epifluoresence microscopy (Figures 3 and 8). A possible explanation for this may due to insufficient PIP2 hydrolysis and IP3 production for Ca^{2+} release from endoplasmic reticulum stores. Although a decrease in PIP2 concentration in the immediate vicinity of the channel would cause diffusion of its bound PIP2 away from the channel binding site resulting in current inhibition and was evident

with TEVC, there was no downstream rise in intracellular Ca^{2+} evident with TEVC or Epifluorescence.

Since GIRK4* current inhibition signified Gq activation, we then proceeded to investigate the concentrations at which RHV-006 and RHV-008 agonism showed saturation, and plot them as a function of serotonin concentration at 1μM. Agonism with RHV-006 appears to saturate by 0.1μM (40% normalized Gq activity) (Figure 5), while agonism with RHV-008 appears to saturate by 10μM (65% normalized Gq activity) (Figure 10). Next, we investigated the concentrations at which the RHV-006 and RHV-008 inhibitory effects on serotonin activity were saturated. The normalized Gq activation (relative to the maximal current inhibition – 100%) was plotted as a function of serotonin concentration. We proceeded to perform a serotonin inhibition dose- response experiment with RHV-006 and determine the apparent affinity of 2AR for serotonin in the *Xenopus* oocyte expression system. The results of the dose- response experiment allow us to extrapolate a likely IC_{50} of approximately 0.1μM (Figure 7). (Additionally, inhibition of 2AR with RHV-008 and 1μM 5-HT seems to saturate at 5uM of RHV-008 (Figure 12).

We then looked at both RHV-006 and RHV-008's effects in the presence of serotonin using calcium imaging. 10μM of RHV-006 and RHV-008 showed a significant decrease in the number of calcium responsive cells (~20%) (Figure 17). The time traces also showed a significant number of unresponsive cells in the presence of both RHV-006/8 and 1μM 5-HT (Figures 16, 17). In addition, the level of response of the responding cells is also decreased. Since a decrease in calcium signals signifies a change at binding at the receptor level, we then proceeded to perform a serotonin inhibition dose- responsive experiment with RHV-008 in the presence of 1μM 5-HT using the HEK293 2AR cell line. Figure 19 nicely shows the progressive

time traces of increasing RHV-008 concentrations in the presence of 1μM 5-HT; the level of

response of these responsive cells decreased starting at 5uM RHV-008. Figure 20 shows that the

IC_{50} of RHV-008 in the presence of 1μM 5-HT lies between 5 and 10μM. It can also be

extrapolated that there are receptor- ligand kinetics involved between RHV-008 and serotonin

binding to 2AR over time. Specifically, the IC_{50} at 85 seconds is $0.5\mu M$, a greater than 10-fold

difference from the IC_{50} at 30 seconds. It is conceivable that in some cases, such as in dynamic

regulation of signal transduction processes, kinetic control prevails rather than affinity control.

The data for analogs RHV-023 and RHV-026 were kindly provided by Jason Younkin

and Peter Drossopoulos. RHV-023 and RHV-026 have 45 and 74% Gq agonism respectively and

consequently seem to be more efficacious agonists than RHV-006 and RHV-008. Both RHV-023

and RHV-026 do not appear to affect serotonin's activity; in fact, RHV-026 seems to have a non-

antagonistic, additive effect on serotonin's activity.

Our two-electrode voltage-clamp assay findings show that all four deconstructed analogs

by themselves have partial Gq activity normalized to basal. However, the Epifluorescence assay

does not show downstream calcium signaling of these compounds. This could be explained by

the greater sensitivity of the TEVC assay at the receptor- channel membrane level, and perhaps

insufficient PIP2 hydrolysis for intracellular calcium release. Next, our findings show that the

addition of 1-(piperidin-1-yl)butane (structure in analogs RHV-023 and RHV-026) (Fig. 1B) to

the piperidine ring and benzisoxazole ring system does not suppress the activity of serotonin, but

the removal of this structure greatly suppresses serotonin's activity. Interestingly, although

RHV-006 and RHV-008 are structurally most similar to serotonin, these analogs instead act

similarly to risperidone. On the other hand, RHV-023 and RHV-026 act the least similarly to

risperidone, but have the most structural similarity. This could be accounted for by the removal of the amine and methyl group from the risperidone molecule.

In conclusion, the smaller compounds, RHV-006/8, are partial agonist by themselves and antagonize the effects of serotonin down to their partial agonism level. The longer compounds, RHV-023/26, are more efficacious agonists than RHV-006/8, but do not display an antagonistic effect on serotonin, unlike compounds RHV-006/8.

Further research is needed to complete deconstructed analogs' dose responses for agonism and antagonism using the TEVC assay. Additionally, further research is needed to complete the same dose responses using the epifluorescence assay. The combined study of these deconstructed analogs using both assays discussed in the present work will give us a better idea of the portion of risperidone that is important to 5HT2AR functional activity and response.

LITERATURE CITED

Ballesteros, Juan A., and Harel Weinstein. "Integrated methods for the construction of three-dimensional models and computational probing of structure-function relations in G protein-coupled receptors." *Methods in neurosciences* 25 (1995): 366-428.

Birnbaumer, Lutz, Joel Abramowitz, and Arthur M. Brown. "Receptor-effector coupling by G proteins." *Biochimica et Biophysica Acta (BBA)-Reviews on Biomembranes* 1031.2 (1990): 163-224.

Crow, Tim J. "Molecular pathology of schizophrenia: more than one disease process?." *BMJ* 280.6207 (1980): 66-68.

Ellenbroek, B. A. "Treatment of schizophrenia: a clinical and preclinical evaluation of neuroleptic drugs." *Pharmacology & therapeutics* 57.1 (1993): 1-78.

Fisman, Sandra and Margaret Steele. "Use of risperidone in pervasive developmental disorders: a case series." *Journal of child and adolescent psychopharmacology* 6.3 (1996): 177-190.

Fribourg, Miguel, et al. "Decoding the signaling of a GPCR heteromeric complex reveals a unifying mechanism of action of antipsychotic drugs."*Cell* 147.5 (2011): 1011-1023.

Gaitonde, Supriya. *Deconstruction of Risperidone: An analysis of its inverse agonism at $5HT_{2A}$ receptors*. Poster session presented at the VCU School of Pharmacy 15th Annual Phamaceutical Science Research and Career Day, November 2013, Richmond, VA.

Glennon, Richard A. "Serotonin Receptor Subtypes and Ligands." *Neuropsychopharmacology: the Fourth Generation of Progress* (2000).

Glennon, Richard A. "Central serotonin receptors as targets for drug research." *Journal of medicinal chemistry* 30.1 (1987): 1-12.

Glennon, R. A. and Dukat, M. Serotonin receptors and drugs affecting serotonergic neurotransmission. In Williams, D. A., Lemke, T. M. (Eds.), *Foye's Principles of Medicinal Chemistry*. Lippincott Williams & Wilkins: Philadelphia, PA. (2002), pp 315- 337.

Glick, Ira D., et al. "Treatment with atypical antipsychotics: new indications and new populations." *Journal of psychiatric research* 35.3 (2001): 187-191.

Hatcher-Solis, Candice, et al. "G Protein-Coupled Receptor Signaling to Kir Channels in Xenopus Oocytes." *Current pharmaceutical biotechnology* 15.10 (2014): 987-995.

Hefner, H. (1993) What is schizophrenia? Neurol Psychiatr Brain. Res 2:36-52

Hibino, Hiroshi, et al. "Inwardly rectifying potassium channels: their structure, function, and physiological roles." *Physiological reviews* 90.1 (2010): 291-366.

Keselman, Inna, et al. "Mechanism of PLC-mediated Kir3 current inhibition." *Channels* 1.2 (2007): 113-123.

Lefkowitz, R. J. "Seven transmembrane receptors: something old, something new." *Acta physiologica* 190.1 (2007): 9-19.

Lin, H. H. "G-protein-coupled receptors and their (Bio) chemical significance win 2012 Nobel Prize in Chemistry." *Biomedical journal* 36.3 (2013): 118.

Marder, Stephen R., John M. Davis, and Guy Chouinard. "The effects of risperidone on the five dimensions of schizophrenia derived by factor analysis: combined results of the North American trials." *J Clin Psychiatry* 58.12 (1997): 538-546.

Megens, A. A. H. P., et al. "Survey on the pharmacodynamics of the new antipsychotic risperidone." *Psychopharmacology* 114.1 (1994): 9-23.

Milligan, Graeme. "Constitutive activity and inverse agonists of G protein-coupled receptors: a current perspective." *Molecular pharmacology* 64.6 (2003): 1271-1276.

Richelson, Elliott, and Terry Souder. "Binding of antipsychotic drugs to human brain receptors: focus on newer generation compounds." *Life sciences* 68.1 (2000): 29-39.

Schotte, An, et al. "Risperidone compared with new and reference antipsychotic drugs: in vitro and in vivo receptor binding." *Psychopharmacology* 124.1-2 (1996): 57-73.

Stevens, Janice R. "An anatomy of schizophrenia?." *Archives of General Psychiatry* 29.2 (1973): 177-189.

Zhang, Gongliang, et al. "Stimulation of serotonin 2A receptors facilitates consolidation and extinction of fear memory in C57BL/6J mice." *Neuropharmacology* 64 (2013): 403-413.